Mono- and Bi-nuclear Hydroxamates of Bis(2-phenylazopyridine)ruthenium(II)

Phalguni Ghosh and Animesh Chakravorty*
Department of Inorganic Chemistry, Indian Association for the Cultivation of Science, Calcutta 700 032, India

The synthesis and characterisation of chelates of types $[Ru(pap)_2\{ON(R)C(O)C_6H_4X\text{-}p\}][ClO_4]\cdot H_2O$, (**1**), $[Ru(pap)_2\{ON{=}C(O)C_6H_4X\text{-}p\}]\cdot H_2O$, (**2**), $[\{Ru(pap)_2\}_2\{ON(R)C(O)\text{–}C(O)N(R)O\}][ClO_4]_2\cdot H_2O$, (**3**), and $[\{Ru(pap)_2\}_2\{ON(R)C(O)\text{–}Y\text{–}C(O)N(R)O\}][ClO_4]_2\cdot H_2O$, (**4**), where pap = 2-phenylazopyridine [R = H, Me, or Ph; X = H, Me, Cl, OMe, or NO_2; Y = p-C_6H_4 or $(CH_2)_4$] are described. The presence of Ru–pap π back bonding and the hydroxamate–hydroximate chelate resonance are demonstrated by i.r. data. All complexes display $t_2(Ru)\rightarrow\pi^*(pap)$ charge-transfer transitions (900—500 nm). Species (**1**) show the reversible ruthenium(III)–ruthenium(II) couple in acetonitrile [1.03—1.17 V *vs.* saturated calomel electrode (s.c.e.), cyclic voltammetry]; for (**2**) the couple shifts to lower potentials by *ca.* 600 mV. The formal potentials are sensitive to substituents on the $ON(R)C(O)C_6H_4X\text{-}p$ and $ON{=}C(O)C_6H_4X\text{-}p$ functions. Complexes (**1**; R = H) act as monobasic acids (pK 5.76—7.65) in water–dioxane(60:40). In one case the electroprotic equilibrium $[Ru(pap)_2L]^+ + H^+ + e^- \rightleftharpoons [Ru(pap)_2(HL)]^+$ [L = $ON{=}C(O)Ph$] ($E_{298}^{\ominus}$ = 0.88 V) has been identified with the help of variable-pH cyclic voltammetry. The binuclear species in general display two successive ruthenium(III)–ruthenium(II) couples. All complexes show azo-reductions on the negative side of the s.c.e.

Hydroxamic acids have been used as analytical reagents for a long time.[1,2] Recent interest in the chemistry and structure of metal hydroxamates emanates from the recognition that hydroxamic acids are potent siderophores in bacterial iron transport.[3,4] So far the hydroxamates of 4*d* and 5*d* elements, unlike those of 3*d* elements,[2,5,6] have received relatively meagre attention.[7–11] Thus, while iron hydroxamates have been of central interest[12–14] virtually nothing is known about the corresponding chemistry of ruthenium and osmium. The reported synthesis of a tris hydroxamate of ruthenium[15] is not reproducible and our search for such chelates continues. Considerable progress has, however, been made with regard to species having a single hydroxamate or hydroximate anion bound to a $[Ru(L\text{–}L)_2]^{n+}$ moiety (L–L = bidentate ligand). Herein we report the synthesis and selected properties of groups of mononuclear and binuclear species of this type having 2-phenylazopyridine, $C_6H_5N{=}NC_5H_4N$ (pap) as the bidentate ligand.

Results and Discussion

Synthesis and Spectra. The complexes reported are of the types $[Ru(pap)_2\{ON(R)C(O)C_6H_4X\text{-}p\}][ClO_4]\cdot H_2O$ (**1**), $[Ru(pap)_2\{ON{=}C(O)C_6H_4X\text{-}p\}]\cdot H_2O$ (**2**), $[\{Ru(pap)_2\}_2\{ON(R)C(O)\text{–}C(O)N(R)O\}][ClO_4]_2\cdot H_2O$ (**3**), and $[\{Ru(pap)_2\}_2\{ON(R)C(O)\text{–}Y\text{–}C(O)N(R)O\}][ClO_4]_2\cdot H_2O$ (**4**). The specific complexes and the identification of R^2, X, and Y are given in Table 1. The dark violet complexes (**1**), (**3**), and (**4**) are furnished in good yield from the reaction of $[Ru(pap)_2(OH_2)_2][ClO_4]_2\cdot H_2O$[14,15] (**5**) with hydroxamic acids in boiling water–ethanol (80:20) [N_p and N_a in (**5**) are respectively the pyridine and azo-nitrogen atoms]. These salts have the expected electrical conductivity in solution (Table 1). The bluish green non-electrolyte complexes (**2**) are prepared by the deprotonation of $[Ru(pap)_2(HL)][ClO_4]\cdot H_2O$ [L = $ON{=}C(O)C_6H_4X\text{-}p$] with NaOH. The deprotonation equilibrium was studied quantitatively (see later). All complexes are diamagnetic.

The above synthetic reactions were carried out in air without any particular precaution. Applications of similar conditions when preparing 2,2′-bipyridine (bipy) analogues (pap replaced by bipy) invariably leads to very impure products contaminated by ruthenium nitrosyl species [ν(NO) at *ca.* 1 800 cm^{-1}] of uncertain nature. We therefore shifted our interest from bipy to pap. Subsequently we have been able[18] to isolate pure hydroxamates of the $Ru(bipy)_2$ moiety using anaerobic low-temperature reaction conditions. The difference in the behaviour of bipy and pap can be rationalised in terms of the stronger π-acceptor character[17,19] of the latter. In effect ruthenium(II) is better stabilised by pap than bipy. The abstraction of the nitrosyl group from hydroxamate is thus suppressed when the pap ligand is present. The low stability of nitrosyls in Ru–pap chemistry is demonstrated by the following observation.[20] The labile complex $[Ru(pap)_2(NO)(NO_2)]^{2+}$ is formed on adding concentrated $HClO_4$ to $[Ru(pap)_2(NO_2)_2]$ in acetonitrile. However, attempted isolation of the nitrosyl complex invariably affords the original dinitro-species. This is in contrast to the case[21] of stable $[Ru(bipy)_2(NO)(NO_2)]^{2+}$.

The complexes display many vibrational frequencies in the i.r. region. One significant observation is the decrease in ν(N=N) stretching frequency in going from free pap (1 425 cm^{-1}) to the complexes (Table 2). This is attributed to the presence of $d(Ru)\rightarrow\pi^*(pap)$ back bonding in the ground state. The azo-stretch is particularly affected since the π*(pap) orbital (lowest occupied molecular orbital, l.u.m.o.) is largely azo in character.[17] The lowering of ν(C=O) (Table 2) compared to the free-ligand values (1 600—1 650 cm^{-1}) is attributed to hydroxamate–hydroximate, (**6a**) ↔ (**6b**), resonance which occurs quite generally among metal hydroxamates.[9–11,22,23] The ν(C=O) values of hydroximate complexes (**2**) are systematically lower than those of (**1**) as expected.

The complexes have several absorption maxima in the region 200—900 nm (Table 2). Two bands systematically appear at *ca.* 660 and *ca.* 560 nm for complexes of type (**1**); large red shifts of these bands occur on going to the deprotonated complexes (**2**) (Figure 1). These are assigned to metal-to-ligand charge-transfer (m.l.c.t.) transitions of the type $d(Ru)\rightarrow\pi^*(pap)$ as in other complexes.[16,17,19,24] The red shift on deprotonation is understandable since proton loss destabilises the metal orbitals due to the increase in ligand (hydroximate) charge and decrease in effective positive charge on the metal. This is also consistent with the decrease in metal redox potential on deprotonation as discussed below.

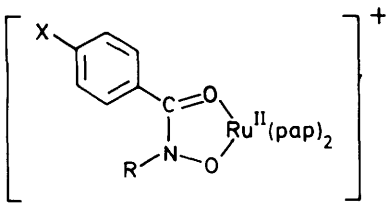

(1)

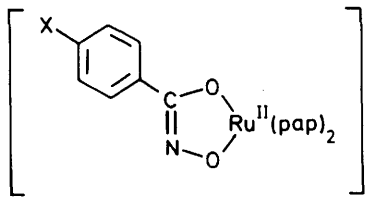

(2)

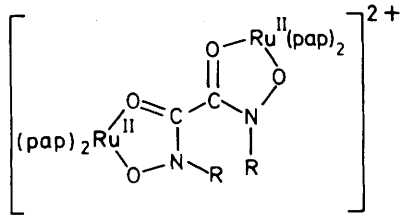

(3)

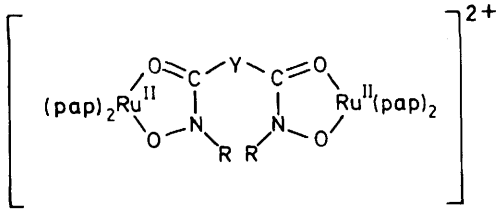

(4)

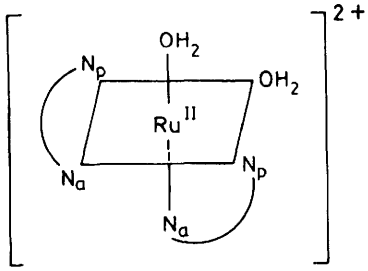

(5)

Electrochemistry.—*Ruthenium*(III)–*ruthenium*(II) *couple.* All complexes of type (**1**) systematically display the ruthenium(III)–ruthenium(II) couple (1) in acetonitrile (Table 3, Figure 2) near

$$[Ru(pap)_2\{ON(R)C(O)C_6H_4X\text{-}p\}]^{2+} + e^- \rightleftharpoons [Ru(pap)_2\{ON(R)C(O)C_6H_4X\text{-}p\}]^{+} \quad (1)$$

1 V *vs.* the saturated calomel electrode (s.c.e.) at platinum or glassy carbon electrodes. The cyclic voltammetric peak-to-peak separation remains nearly constant at 60—70 mV up to a scan rate of 1 V s^{-1} showing that the electrode process is reversible.

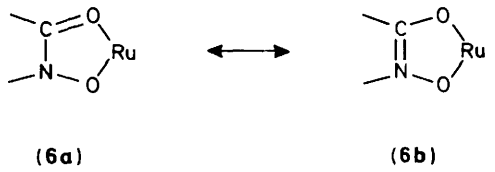

(6a) (6b)

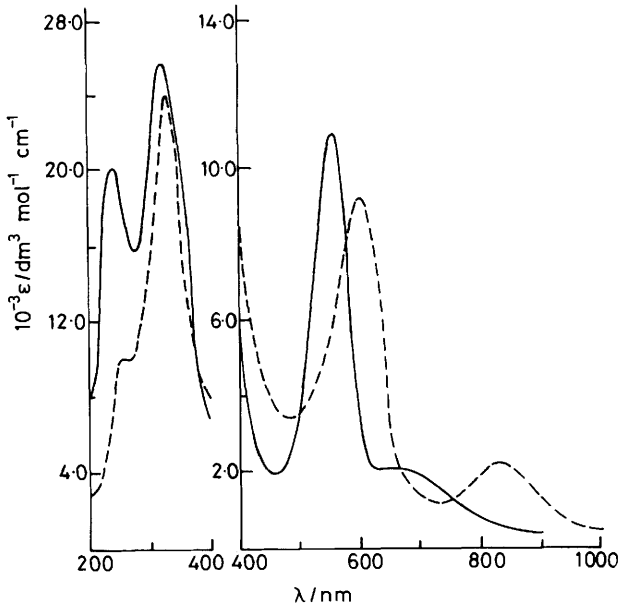

Figure 1. Electronic spectra of complex (**1k**) (——) and (**2a**) (— — —) in acetonitrile solution

The one-electron couple (1) was confirmed coulometrically (Table 3). The oxidised solutions are unstable and decompose to products which could not be reduced back to the original species.

For the deprotonated complexes (**2**) the reversible metal redox couple (2) occurs near 0.4 V (Table 3, Figure 2). The

$$[Ru(pap)_2\{ON{=}C(O)C_6H_4X\text{-}p\}]^{+} + e^- \rightleftharpoons [Ru(pap)_2\{ON{=}C(O)C_6H_4X\text{-}p\}] \quad (2)$$

dramatic potential shift in going from (**1**) to (**2**) is consistent with the destabilisation of metal orbitals (see above) on deprotonation.

Hammett correlation. The formal potential, $E_{298}^{\ominus}$, of couple (1) increases in the following order of R for a given X: Me < H < Ph. For a given R the potential correlates linearly with the Hammett substituent constant, σ, of X (Figure 3). The $E_{298}^{\ominus}$ values of couple (2) behave similarly but the reaction constant ρ is significantly larger (Figure 3). The effect of the polar substituent is better transmitted on deprotonation.

Ligand reduction. In the case of complexes (**1**) with R = Me or Ph up to three successive reductions are observed on the negative side of the s.c.e. at a glassy carbon electrode. The reduction at lowest potential involves two electrons whereas the other two have one-electron stoicheiometry (Table 3, Figure 2). These are assigned to azo reduction [17] [couples (3) and (4)]. For

$$-N{=}N- + e^- \rightleftharpoons -N^{\cdot\cdot\cdot}N-^{-} \quad (3)$$

$$-N^{\cdot\cdot\cdot}N-^{-} + e^- \rightleftharpoons -N\text{–}N-^{2-} \quad (4)$$

Table 1. Microanalytical[a] (%) and conductivity[b] data for complexes (1)—(4)

Complex			Λ_M/Ω^{-1} cm^2 mol^{-1}	Analysis/%			
	R	X		C	H	N	Cl
(1a)	Me	OMe	135	48.7 (48.6)	4.0 (3.9)	12.7 (12.8)	4.6 (4.6)
(1b)	Me	Me	120	49.6 (49.7)	4.1 (4.0)	13.2 (13.1)	4.7 (4.7)
(1c)	Me	H	140	48.9 (49.0)	3.9 (3.8)	13.4 (13.3)	4.8 (4.8)
(1d)	Me	Cl	125	46.9 (46.8)	3.6 (3.5)	12.7 (12.7)	9.3 (9.2)
(1e)	Me	NO_2	145	46.3 (46.2)	3.6 (3.5)	14.3 (14.3)	4.7 (4.6)
(1f)	Ph	OMe	130	52.3 (52.2)	4.1 (3.9)	11.8 (11.9)	4.3 (4.3)
(1g)	Ph	Me	125	53.3 (53.2)	4.1 (4.0)	12.1 (12.0)	4.4 (4.3)
(1h)	Ph	H	140	52.7 (52.7)	4.0 (3.9)	12.3 (12.3)	4.5 (4.5)
(1i)	Ph	Cl	155	50.8 (50.9)	3.7 (3.6)	11.7 (11.8)	8.6 (8.5)
(1j)	Ph	NO_2	150	49.9 (49.8)	3.6 (3.5)	11.3 (11.3)	4.3 (4.2)
(1k)	H	OMe	145	47.9 (48.0)	4.1 (4.0)	13.1 (13.0)	4.7 (4.7)
(1l)	H	Me	140	48.9 (49.0)	3.9 (3.8)	13.4 (13.3)	4.9 (4.8)
(1m)	H	H	125	48.4 (48.3)	3.7 (3.6)	13.7 (13.6)	4.8 (4.9)
(1n)	H	Cl	140	46.1 (46.1)	3.5 (3.3)	12.9 (12.9)	9.4 (9.4)
(1o)	H	NO_2	150	45.4 (45.4)	3.3 (3.2)	14.7 (14.6)	4.7 (4.6)
(2a)		OMe	*c*	55.4 (55.4)	4.3 (4.1)	15.1 (15.1)	
(2b)		Me	*c*	56.7 (56.8)	4.4 (4.3)	15.6 (15.5)	
(2c)		H	*c*	56.3 (56.1)	4.2 (4.0)	15.9 (15.8)	
(2d)		Cl	*c*	53.3 (53.2)	3.8 (3.7)	14.8 (14.9)	5.3 (5.4)
(2e)		NO_2	*c*	52.4 (52.3)	3.8 (3.6)	16.8 (16.8)	
(3a)	H		270	43.4 (43.5)	3.2 (3.1)	15.6 (15.4)	5.7 (5.6)
(3b)	Ph		280	48.9 (49.0)	3.3 (3.4)	13.9 (13.8)	5.1 (5.0)
(4a)	H	(Y = *p*-C_6H_4)	260	46.5 (46.4)	3.4 (3.3)	14.7 (14.6)	5.4 (5.3)
(4b)	Ph	[Y = $(CH_2)_4$]	240	50.5 (50.4)	3.9 (3.8)	13.4 (13.3)	4.9 (4.8)

[a] Calculated data are in parentheses. [b] In MeCN at 298 K. [c] Non-electrolyte.

Table 2. Selected i.r.[a] and electronic[b] spectral data for the complexes

Complex	I.r. (cm^{-1})		U.v.–visible, λ/nm (ε/dm^3 mol^{-1} cm^{-1})
	ν(N=N)	ν(CO)	
(1a)	1 315	1 590	665(2 100), 562(15 500), 320(28 300), 240(21 000)
(1b)	1 320	1 595	660(2 300), 560(13 800), 320(23 900), 250(12 600)
(1c)	1 315	1 590	670(1 500), 560(13 100), 320(23 400), 240(19 000)
(1d)	1 320	1 595	660(1 800), 560(12 200), 320(25 400), 240(20 600)
(1e)	1 315	1 590	665(1 600), 560(12 300), 320(25 600), 250(21 500)
(1f)	1 315	1 605	650(1 400), 560(9 700), 320(24 100), 260(24 000)
(1g)	1 310	1 595	660(1 500), 560(12 800), 320(26 800), 240(23 300)
(1h)	1 320	1 600	650(1 500), 560(12 000), 315(23 900), 245(26 900)
(1i)	1 310	1 610	655(2 000), 555(9 200), 310(19 900), 250(21 400)
(1j)	1 315	1 595	650(2 100), 560(15 200), 320(36 700), 245(30 600)
(1k)	1 320	1 590	655(2 000), 560(11 000), 320(25 600), 245(20 000)
(1l)	1 310	1 595	660(1 900), 565(10 200), 320(24 300), 245(22 200)
(1m)	1 320	1 590	660(1 400), 570(9 000), 320(28 300), 245(18 900)
(1n)	1 310	1 585	660(1 400), 560(11 200), 320(29 400), 240(20 200)
(1o)	1 320	1 595	665(1 800), 560(12 400), 320(26 400), 245(24 000)
(2a)	1 330	1 570	835(2 000), 600(7 200), 330(24 000), 255(10 000)
(2c)	1 330	1 570	830(2 000), 605(9 900), 325(35 800), 260(15 000)
(2d)	*c*	*c*	830(1 700), 600(9 000), 330(36 000), 260(14 000)
(2e)	1 325	1 580	825(1 800), 600(9 500), 325(28 500), 260(11 500)
(3a)	1 320	1 590	660(1 500), 570(10 400), 320(30 000), 245(20 000)
(3b)	1 320	1 580	650(1 600), 560(13 000), 315(25 000), 245(27 000)
(4a)	1 315	1 590	655(1 800), 560(12 200), 320(26 000), 245(21 000)
(4b)	1 320	1 600	660(2 000), 570(13 200), 320(28 000), 245(20 000)

[a] KBr disc, 4 000—400 cm^{-1}; ν(N=N), strong and sharp; ν(CO), very strong and broad. [b] In MeCN at 298 K. [c] Measurements not made.

two azo-groups four one-electron responses are expected of which the last two are superimposed. For complexes (**1**) with R = H only the first azo-reduction is clearly observed.

The deprotonated complexes (**2**) are reduced with more difficulty than (**1**). This is expected since the extra charge on the hydroximate ligand hinders electron addition to neighbouring pap ligands.

Bridged dimers. Cyclic voltammetric results are given in Table 4 and Figure 4. Complexes (**3a**) and (**3b**) display two overlapping but distinct ruthenium(III)–ruthenium(II) couples (5a) and (5b). The presence of significant ligand-mediated metal–metal

$$[Ru^{III}\{ON(R)C(O)\text{–}C(O)N(R)O\}Ru^{III}]^{4+} + e^- \rightleftharpoons [Ru^{III}\{ON(R)C(O)\text{–}C(O)N(R)O\}Ru^{II}]^{3+} \quad (5a)$$

$$[Ru^{III}\{ON(R)C(O)\text{–}C(O)N(R)O\}Ru^{II}]^{3+} + e^- \rightleftharpoons [Ru^{II}\{ON(R)C(O)\text{–}C(O)N(R)O\}Ru^{II}]^{2+} \quad (5b)$$

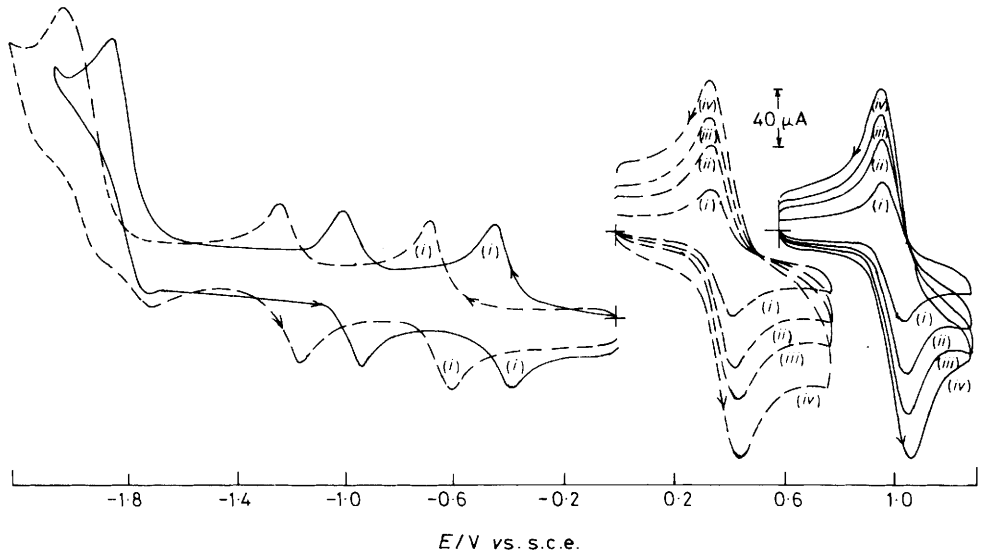

Figure 2. Cyclic voltammograms of complexes (**1c**) (——) and (**1m**) (— — —) in acetonitrile (0.1 mol dm^{-3} $[NEt_4][ClO_4]$) at scan rates (*i*) 50, (*ii*) 200, (*iii*) 500, and (*iv*) 1 000 mV s^{-1}. The working electrodes are respectively platinum and glassy carbon above and below 0.0 V

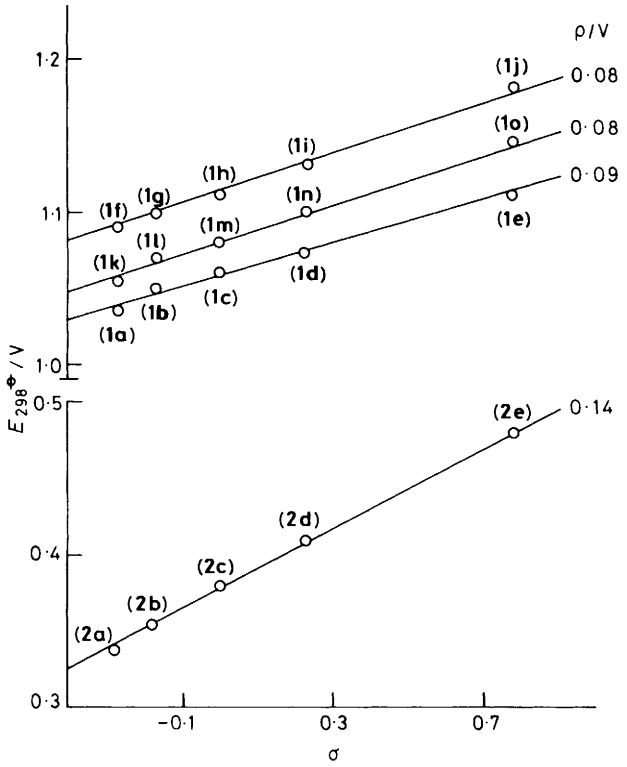

Figure 3. Least-squares plots of $E_{298}^{\ominus}$ *versus* σ

interaction in each case is thus demonstrated. In both complexes (**4a**) and (**4b**) the bridge donor atoms are separated by the same number of carbon atoms, yet the latter unlike the former behaves as though it has two independent and isolated ruthenium atoms [couple (6)]. The aromatic ring in (**4a**) mediates metal–metal interaction much better than does the aliphatic chain in (**4b**). This effect becomes even more evident on comparing the results for complex (**3**) with those for (**4a**).

$$[Ru^{III}\{ON(R)C(O)\text{–}Y\text{–}C(O)N(R)O\}Ru^{III}]^{4+} + 2e^- \rightleftharpoons [Ru^{II}\{ON(R)C(O)\text{–}Y\text{–}C(O)N(R)O\}Ru^{II}]^{2+} \quad (6)$$

Table 3. Cyclic voltammetric data[a]

	Ru^{III}–Ru^{II} couple[b]		pap reduction[d]		
	$E_{298}^{\ominus}$/V	n[c]	$-E_{298}^{\ominus}$/V (ΔE_p/mV)		
(**1a**)	1.03	0.98	0.44 (60),	0.98 (60),	1.83 (130)
(**1b**)	1.05	*e*	0.44 (60),	0.98 (70),	1.83 (140)
(**1c**)	1.06	1.01	0.42 (60),	0.97 (60),	1.82 (150)
(**1d**)	1.07	*e*	0.42 (60),	0.98 (60),	1.82 (130)
(**1e**)	1.10	0.97	0.41 (60),	*f*,	1.80 (140)
(**1f**)	1.08	1.02	0.42 (60),	1.07 (70),	1.89 (90)
(**1g**)	1.10	*e*	0.42 (60),	1.06 (70),	1.88 (100)
(**1h**)	1.11	1.05	0.41 (60),	1.06 (70),	1.88 (100)
(**1i**)	1.13	*e*	0.41 (60),	1.05 (60),	1.89 (120)
(**1j**)	1.17	0.99	0.40 (60),	*f*,	1.86 (100)
(**1k**)	1.05	1.00	0.42 (60),	*g*,	*g*
(**1l**)	1.07	*e*	0.42 (60),	*g*,	*g*
(**1m**)	1.08	1.02	0.41 (60),	*g*,	*g*
(**1n**)	1.10	*e*	0.40 (60),	*g*,	*g*
(**1o**)	1.14	1.04	0.39 (60),	*f*,	*g*
(**2a**)	0.33	0.96	0.65 (60),	1.19 (60),	1.95 (100)
(**2b**)	0.35	*e*	0.64 (60),	1.18 (60),	1.93 (120)
(**2c**)	0.38	0.98	0.63 (60),	1.18 (60),	1.19 (120)
(**2d**)	0.41	*e*	0.63 (60),	1.15 (60),	1.90 (110)
(**2e**)	0.48	0.97	0.60 (60),	*f*,	1.88 (120)

[a] Meaning of symbols as in text; unless otherwise stated all measurements were made in MeCN at a platinum working electrode using 0.1 mol dm^{-3} $[NEt_4][ClO_4]$ as supporting electrolyte. [b] From cyclic voltammetry: $E_{298}^{\ominus}$ calculated as the averages of the cathodic and anodic peak potentials: scan rates 50 mV s^{-1}—1 V s^{-1}; ΔE_p = 60—70 mV over the entire range of scan rates. [c] $n = Q/Q'$ where Q' is the calculated coloumb count for one-electron transfer and Q is the coloumb count found after exhaustive coloumetric oxidation using a platinum-wire gauge at 1.3 V for species (**1**) and at 0.7 V for species (**2**). [d] Glassy carbon electrode: scan rate 100 mV s^{-1}. [e] Measurements not made. [f] Due to the presence of NO_2 reduction the voltammograms are not well characterised. [g] Ill defined voltammograms.

Although the oxidised complexes are stable on the cyclic voltammetric time-scale, they decompose on longer time scales (see above) and we have not been able to isolate and characterise the mixed-valence species. The conproportionation

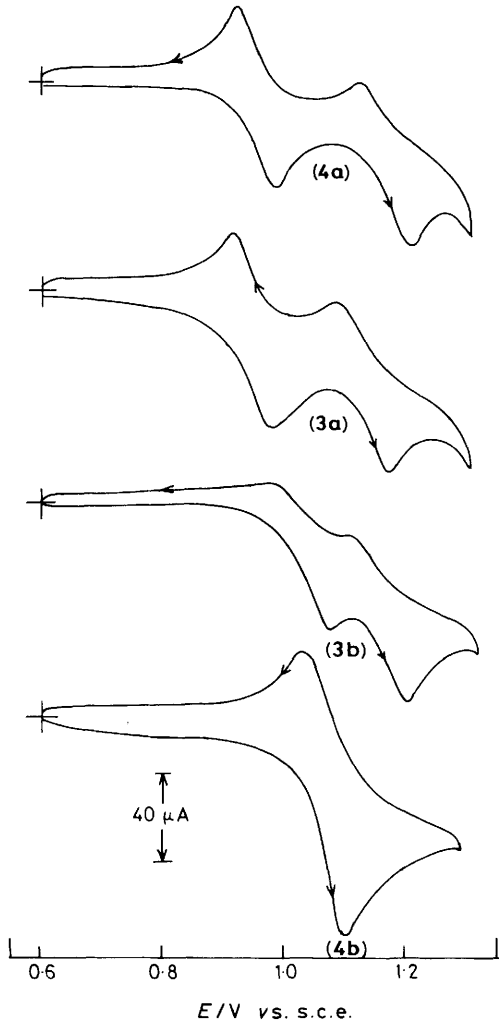

Figure 4. Cyclic voltammograms of complexes (**3a**), (**3b**), (**4a**), and (**4b**) at scan rate 50 mV s^{-1} in acetonitrile (0.1 mol dm^{-3} $[NEt_4][ClO_4]$) with a platinum working electrode

constant,[25] K_c, for reaction (7) (L = bridging ligand) can still be estimated from the difference ($\Delta E_{298}^{\ominus}$) between the cyclic

$$[Ru^{III}LRu^{III}]^{4+} + [Ru^{II}LRu^{II}]^{2+} \overset{K_c}{\rightleftharpoons} 2[Ru^{III}LRu^{II}]^{3+} \quad (7)$$

voltammetric formal potentials of couples like (5a) and (5b). The magnitudes of K_c are: (**3a**), 10^3; (**3b**), 10^2; (**4a**), 10^4. The K_c values are not given any more precisely since small experimental errors in $\Delta E_{298}^{\ominus}$ are magnified exponentially in K_c.

No other examples of the bridging of two $Ru^{II}(pap)_2$ moieties by organic ligands are known at present; the bipy analogues of complexes (**3**) and (**4**) are also unknown. In nitrogen donor-bridged $Ru^{II}(bipy)_2$ dimers the differences between the $E_{298}^{\ominus}$ values of the two ruthenium(III)–ruthenium(II) couples lie in the range [26–30] 0—400 mV depending on the nature and size of the bridge.

Protic and electroprotic equilibria. Metal oxidation is expected to augment the acidity of protons of bound ligands.[31] We have probed this phenomenon with the help of potentiometry and cyclic voltammetry in water–dioxane (60:40).

The pK values for equilibrium (8) were determined pH-

Table 4. Ruthenium(III)–ruthenium(II) formal potentials for the binuclear species. Cyclic voltammetry was carried out in MeCN and 0.1 mol dm^{-3} $[NEt_4][ClO_4]$ as supporting electrolyte

Complex	$E_{298}^{\ominus}$/V (ΔE_p/mV)
(**3a**)	0.94 (70), 1.13 (80)
(**3b**)	1.01 (90), 1.16 (90)
(**4a**)	0.95 (70), 1.17 (80)
(**4b**)	1.07 (70)

Table 5. pK Values of complexes (**1**). Meaning of symbols as in text. Measurements were made in water–dioxane (60:40) (in 1 mol dm^{-3} NaCl); solute concentration *ca.* 10^{-2} mol dm^{-3}

Complex	pK ($\pm$0.05)
(**1k**)	7.65
(**1l**)	7.45
(**1m**)	7.15
(**1n**)	6.70
(**1o**)	5.76

Table 6. Variable-pH cyclic voltammetric results[a] for complex (**1m**) at a glassy carbon electrode in water–dioxane buffers (60:40)

pH	$\bar{E}_p$/V (ΔE_p/mV)	$E_{298}^{\ominus}$[b]/V
1.50	0.80 (100)	0.89
2.45	0.74 (120)	0.88
4.66	0.62 (90)	0.89
5.45	0.56 (100)	0.88
8.64	0.46 (90)	0.46
11.15	0.46 (90)	0.46

[a] Meaning of symbols as in text. Solute concentration 0.1 mol dm^{-3}; scan rate 100 mV s^{-1}. [b] Calculated with the help of the equation $E_{298}^{\ominus} = \bar{E}_p + 0.059$ pH.

$$[Ru(pap)_2(HL)]^{+} \overset{K}{\rightleftharpoons} [Ru(pap)_2L] + H^{+} \quad (8)$$

metrically for all the five available HL species [L = ON=C(O)C_6H_4X-*p*]. There is a marked increase in acidity when X becomes more electron withdrawing (Table 5). A plot of pK *vs.* σ of X is an excellent straight line obeying equation (9) where

$$\Delta pK = -1.8\sigma \quad (9)$$

ΔpK is the change of pK in going from X = H to X = X. We note that $[Ru(bipy)_2(HL)]^{+}$ is a weaker[18] acid than $[Ru(pap)_2(HL)]^{+}$ [L = ON=C(O)Ph] by almost three orders of magnitude due to the higher π acidity[16] of pap.

The ruthenium(III) species $[Ru(pap)_2(HL)]^{2+}$ or $[Ru(pap)_2L]^{+}$ could not be isolated due to their instability (see above) and no direct assessment of pK is possible. However, an estimate of the strong acidity of $[Ru(pap)_2(HL)]^{2+}$ can be made using variable-pH cyclic voltammetric data as illustrated in the case of the HL complex [L = ON=C(O)Ph] which was studied in the range pH 1—12. Results are in Table 6 and Figure 5.

Examination of formation curves as a function of pH shows that above pH 8 $[Ru(pap)_2L]$ [L = ON=C(O)Ph] alone contributes to solution composition. On the other hand at pH < 6 the entire complex is present as $[Ru(pap)_2(HL)]^{+}$. The cyclic voltammograms of $[Ru(pap)_2(HL)]^{+}$ indeed became pH independent above pH 8 (Table 6). The response is merely that due to couple (2). The formal potential (0.46 V) in water–dioxane (60:40) is higher than that in acetonitrile. Below pH 6 the peak potential shifts at the rate of 60 mV per unit change of pH (Table 6, Figure 5). Clearly both an electron and a proton are being transferred and the electroprotic equilibrium (10) is

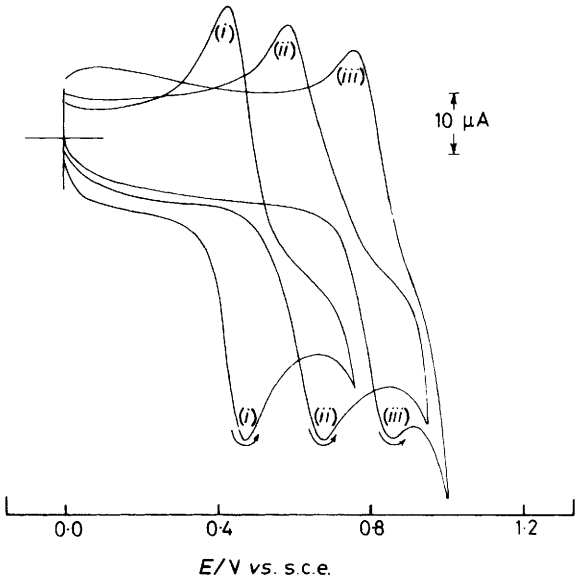

Figure 5. Variable-pH cyclic voltammograms of complex (**1m**) in water–dioxane (60:40) at a glassy carbon electrode and scan rate 100 mV s^{-1} with pH (i) 8.64, (ii) 4.66, and (iii) 1.50

$$[Ru(pap)_2L]^+ + e^- + H^+ \rightleftharpoons [Ru(pap)_2(HL)]^+ \quad (10)$$

operative. In effect the ruthenium(III) complex spontaneously deprotonates because of higher acidity. Since this applies even at a pH as low as 1.5 (Table 6) it is estimated that $[Ru(pap)_2(HL)]^{2+}$ has $pK < 1$.

The formal potential of couple (10) can be calculated with the help of equation (11) where $\bar{E}_p$ is the average cathodic and

$$E_{298}^{\ominus} = \bar{E}_p + 0.059\ pH \quad (11)$$

anodic peak potential. Results are in Table 6. By combining equations (2), (8), and (10), equation (12) can be derived[32]

$$E_{298}^{\ominus}(10) = E_{298}^{\ominus}(2) + 0.059\ pK \quad (12)$$

where $E_{298}^{\ominus}$ (2) and $E_{298}^{\ominus}$ (10) are respectively the formal potentials of couples (2) and (10). Applying $pK = 7.15$ and $E_{298}^{\ominus}$ (10) = 0.88 V, the formal potential of couple (2) is calculated to be 0.46 V in excellent agreement with the experimental value (Table 6).

Conclusions

Mono- and bi-nuclear hydroxamate and hydroximates of $[Ru(pap)_2]^{2+}$ have been isolated in the pure state. Characteristic spectral features are: (1) low ν(N=N) [due to $t_2(Ru) \rightarrow \pi^*(pap)$ back bonding] and ν(C=O) (due to hydroxamate ↔ hydroximate resonance) frequencies and (2) m.l.c.t. transitions in the visible region. For all complexes metal oxidation and multiple ligand (azo-group of pap) reduction couples are systematically observed. With $[Ru(pap)_3]^{2+}$ the ruthenium(III)–ruthenium(II) couple has $E_{298}^{\ominus}$ of 2.10 V.[17] Substitution of one pap by $ON(R)C(O)C_6H_4X$-*p* shifts the potentials by *ca.* 1.0 V to lower values. In the case of substitution by $ON{=}C(O)C_6H_4X$-*p* there is a further downward shift of *ca.* 600 mV. In fact the $[Ru(pap)_2L]$ species have the lowest $E_{298}^{\ominus}$ values among all reported complexes of $[Ru(pap)_2]^{2+}$. All binuclear complexes except (**4b**) display two successive ruthenium(III)–ruthenium(II) couples (separation of $E_{298}^{\ominus}$ values *ca.* 200 mV) showing the presence of ligand-mediated metal–metal interaction. The aromatic ring of complex (**4a**) is the best mediator while the $(CH_2)_4$ bridge in (**4b**) is the poorest. The $[Ru(pap)_2(HL)]^+$ [L = $ON{=}C(O)C_6H_4X$-*p*] complexes acts as monobasic acids (p*K* 7.65—5.76). Like the $E_{298}^{\ominus}$ values of the ruthenium(III)–ruthenium(II) couple, the p*K* value correlates linearly with the Hammett substituent constant (σ) of X. It is indirectly estimated that the ruthenium(III) complex $[Ru(pap)_2\{ON(H)C(O)Ph\}]^{2+}$ is strongly acidic ($pK < 1$) in water–dioxane (60:40). The electroprotic equilibria (10) ($E_{298}^{\ominus} = 0.88$ V) operates in this solvent below pH 6. Attempts to synthesise tris hydroxamates and thiohydroxamates of ruthenium will now be made.

Experimental

Starting Materials.—Published methods[16,24] were used to prepare 2-phenylazopyridine and $[Ru(pap)_2(OH_2)_2][ClO_4]_2 \cdot H_2O$. Different types of monohydroxamic and dihydroxamic acids were prepared by literature methods.[7,33] The purification of solvents and preparation of supporting electrolytes for electrochemical work were done as before.[34] Water of high purity was obtained by distillation of deionised water from $KMnO_4$. Sodium chloride for pH-metric work was recrystallised from water.

Physical Measurements.—Electronic and i.r. spectra were recorded using Cary 17D or Pye-Unicam SP8-150 and Beckman IR-20A spectrophotometers respectively. Solution electrical conductivity was measured using a Philips PR9500 bridge with a solute concentration of *ca.* 10^{-3} mol dm^{-3}. Cyclic voltammetry was performed under a dinitrogen atmosphere with the help of PAR model 370-4 electrochemistry system as before.[11,16,17] In the three-electrode configuration either a Beckman model 39273 platinum electrode or a PAR model G0021 glassy carbon electrode was the working electrode. For controlled-potential coulometry a 173 potentiostat, 179 digital coulometer, and 377A cell system having a platinum-wire-gauge electrode were used. All measurements were made at 298 K. The potentials are referenced to the saturated calomel electrode and are uncorrected for the junction potential.

The following σ values[35] for *para* substituents X were used: OMe, −0.27; Me, −0.17; H, 0.00; Cl, +0.23; NO_2, +0.78.

For the pH-dependent electrochemical measurements, acetate (pH 0.65—5.20), phosphate (pH 5.70—7.55), and borate (pH 7.8—10.0) buffers were used. The voltammograms were recorded in buffer–dioxane (60:40) mixtures. The pH of each mixture was recorded with the help of a Systronics (India) 335 model pH-meter (accurate to ±0.01 pH unit). The electrolytes in their buffers also acted as supporting electrolytes.

*Determination of p*K *Values.*—The determination of p*K* was carried out on 10^{-2} mol dm^{-3} $[Ru(pap)_2(HL)][ClO_4]\cdot H_2O$ [L = $ON{=}C(O)C_6H_4X$-*p*] (10 cm^3) in water–dioxane (60:40) (ionic strength of the solution maintained at 1.0 mol dm^{-3} with NaCl) thermostatted at 298 K. Carbonate-free[36] sodium hydroxide solution (0.0369 mol dm^{-3}) was added from a burette that could be read accurately to 0.01 cm^3. For equilibrium (8), equation (13) holds[37] where *a* is the total concentration of the

$$pK = pH - \log \frac{[Na^+]}{a - [Na^+]} \quad (13)$$

complexes, $[Na^+]$ is the concentration of Na^+ ions from added NaOH, and *K* is the equilibrium constant of reaction (8). The p*K* values were calculated at various levels of neutralisation.

Synthesis of Compounds.—$[Ru(pap)_2\{ON(R)C(O)C_6H_4X$-*p*$\}][ClO_4]\cdot H_2O$. These complexes were synthesised by the general procedure described below.

To a solution of $[Ru(pap)_2(OH_2)_2][ClO_4]_2 \cdot H_2O$ (100 mg, 0.14 mmol) in warm ethanol–water (1:4) (50 cm^3) was added the hydroxamic acid (0.18 mmol). The reaction mixture was heated under reflux for 3 h. Its volume was then reduced to *ca.* 10 cm^3 by evaporation on a water-bath. Dark violet crystals resulted which were filtered off whilst still hot. The residue was washed with a minimum amount of cold water and finally with diethyl ether. The compound was dried *in vacuo* over P_4O_{10}. Yield 80%.

The binuclear complexes were prepared similarly using the appropriate dihydroxamic acids. The reaction time was increased to 10 h.

$[Ru(pap)_2\{ON{=}C(O)C_6H_4X\text{-}p\}] \cdot H_2O$. Freshly prepared $[Ru(pap)_2(HL)][ClO_4] \cdot H_2O$ (0.14 mmol) was dissolved in boiling water (50 cm^3) and stirred magnetically. Sodium hydroxide (5 cm^3, 4.0 mol dm^{-3}) was added and stirring was continued for another 20 min. The bluish green compound was extracted with thiophene-free benzene (10 × 5 cm^3) from cold solution. The volume of the extract was reduced to *ca.* 10 cm^3 by evaporation on a water-bath. The concentrated extract was then mixed with hexane (50 cm^3). The solid compound that separated was filtered off, thoroughly washed with hexane, and then dried *in vacuo* over P_4O_{10}. Yield 90%.

Acknowledgements

We thank the Department of Science and Technology and the Council of Scientific and Industrial Research, Government of India, New Delhi, for financial support.

References

1 A. K. Majumder, 'N-Benzoyl Phenylhydroxylamine and its Analogues,' International Series of Monographs in Analytical Chemistry, vol. 50, Pergamon Press, London, 1971.
2 B. Chatterjee, *Coord. Chem. Rev.*, 1978, **26**, 281.
3 J. B. Neilands (ed.), 'Microbial Iron Metabolism,' Academic Press, New York, 1974.
4 K. N. Raymond, *Adv. Chem. Ser.*, 1977, **162**; G. B. Wong, M. J. Kappel, K. N. Raymond, B. Matzanke, and G. Winkelman, *J. Am. Chem. Soc.*, 1983, **105**, 810.
5 L. A. Dominey and K. Kurtin, *Inorg. Chem.*, 1983, **23**, 103.
6 K. Abu-Dari, S. J. Barclay, P. E. Riley, and K. N. Raymond, *Inorg. Chem.*, 1983, **22**, 3085.
7 L. W. Jones and C. D. Hurd, *J. Am. Chem. Soc.*, 1921, **43**, 2422; S. P. Bag and S. Lahiri, *J. Inorg. Nucl. Chem.*, 1976, **38**, 1611.
8 R. L. Dutta and B. Chatterjee, *J. Indian Chem. Soc.*, 1967, **44**, 780.
9 K. Weighardt, W. Holzbach, E. Hafer, and J. Weiss, *Inorg. Chem.*, 1981, **20**, 343.
10 G. A. Brewer and E. Sinn, *Inorg. Chem.*, 1981, **20**, 1823.
11 P. Ghosh and A. Chakravorty, *Inorg. Chem.*, 1983, **22**, 1322.
12 K. Abu-Dari, C. J. Cooper, and K. N. Raymond, *Inorg. Chem.*, 1978, **17**, 3394; C. J. Carrano, K. N. Raymond, and W. R. Harris, *J. Am. Chem. Soc.*, 1979, **101**, 2722; K. N. Raymond and C. J. Carrano, *Acc. Chem. Res.*, 1979, **12**, 183; S. R. Cooper, J. V. McArdle, and K. N. Raymond, *Proc. Natl. Acad. Sci. USA*, 1978, **75**, 3551.
13 P. Ghosh and A. Chakravorty, *Inorg. Chim. Acta*, 1981, **56**, L77.
14 D. A. Brown and B. S. Sekhon, *Inorg. Chim. Acta*, 1984, **19**, 103.
15 R. S. Mishra, *J. Indian Chem. Soc.*, 1967, **44**, 400; 1969, **46**, 1074.
16 S. Goswami, A. R. Chakravarty, and A. Chakravorty, *Inorg. Chem.*, 1983, **22**, 602.
17 S. Goswami, R. N. Mukherjee, and A. Chakravorty, *Inorg. Chem.*, 1983, **22**, 2825.
18 P. Ghosh and A. Chakravorty, *Inorg. Chem.*, 1984, **23**, 2242.
19 R. A. Krause and K. Krause, *Inorg. Chem.*, 1980, **19**, 2600.
20 S. Goswami and A. Chakravorty, unpublished work.
21 J. B. Godwin and T. J. Veyes, *Inorg. Chem.*, 1971, **10**, 471.
22 W. L. Smith and K. N. Raymond, *J. Am. Chem. Soc.*, 1981, **103**, 3341.
23 K. Abu-Dari and K. N. Raymond, *Inorg. Chem.*, 1980, **19**, 2034.
24 S. Goswami, A. R. Chakravarty, and A. Chakravorty, *Inorg. Chem.*, 1981, **20**, 2246.
25 D. E. Richardson and H. Taube, *Inorg. Chem.*, 1981, **20**, 1278.
26 S. A. Adeyemi, J. N. Braddock, G. M. Brown, J. A. Ferguson, F. J. Miller, and T. J. Meyer, *J. Am. Chem. Soc.*, 1972, **94**, 300.
27 R. W. Callahan, F. R. Keene, T. J. Meyer, and D. J. Salman, *J. Am. Chem. Soc.*, 1977, **99**, 1064.
28 D. Sedney and A. Ludi, *Inorg. Chim. Acta*, 1981, **47**, 153.
29 M. J. Powers and T. J. Meyer, *Inorg. Chem.*, 1978, **17**, 2955.
30 B. P. Sullivan, D. J. Salman, T. J. Meyer, and J. Peedin, *Inorg. Chem.*, 1979, **18**, 3369.
31 J. G. Mohanty and A. Chakravorty, *Inorg. Chem.*, 1976, **15**, 2912; A. N. Singh and A. Chakravorty, *ibid.*, 1980, **19**, 969; H. Beinert, *Coord. Chem. Rev.*, 1980, **33**, 55.
32 J. G. Mohanty and A. Chakravorty, *Inorg. Chem.*, 1977, **16**, 1561.
33 C. R. Hanser and W. B. Renfrow, jun., 'Organic Synthesis,' Col. vol. 2, John Wiley, New York, 1947; H. L. Yale, *Chem. Rev.*, 1944, **33**, 209.
34 R. N. Mukherjee, O. A. Rajan, and A. Chakravorty, *Inorg. Chem.*, 1982, **21**, 785.
35 L. P. Hammett, 'Physical Organic Chemistry,' 2nd edn., McGraw-Hill, New York, 1970.
36 A. I. Vogel, 'Quantitative Inorganic Analysis,' Longmans, Green and Co., London, 1953, p. 177.
37 A. Albert and E. P. Sergeant, 'Ionization Constants of Acids and Bases,' Methuen, London, 1962, p. 30.

Received 26th March 1984; *Paper* 4/496